Cyclic Stress – Strain Behaviour of Styrene Butadiene Rubber (SBR) – Carbon Black–silica Dual phase filler Composites.

M.H. Abd-El Salam[1], M. Mohsen[2]& A. Ismail[1]

[1] *Physics Department, Faculty of Education, Ain Shams University, Cairo, Egypt.*

[2] *Physics Department, Faculty of Science, Ain Shams University, Cairo, Egypt.*

Cyclic stress–strain behaviour of carbon black – silica – styrene butadiene rubber (SBR) composites has been studied at room temperature. It was found that, the hysteresis in SBR – carbon black composites is more pronounced than in SBR – silica composites and the elastic recovery (E_R) was found to be dependent on the filler type and content. The obtained stress – strain data for the tested samples were fitted in view of the molecular statistical model of rubber elasticity, taking into account the generalized non-Gaussian tube model of finite network extensibility with a topological constraint contribution and the damage model of stress-induced filler cluster breakdown. The experimental results were confirmed by using electron micrographs to show the filler clusters.

1. Introduction:

Polymer blends and composites are widely used in different technological purposes because of their high strength, high elastic deformability, and the ability to be strained repeatedly to high levels without destruction or permanent distortion. For many uses, even vulcanized rubbers do not exhibit satisfactory tensile strength, modulus, hardness, abrasion resistance, and tear resistance. These properties can be enhanced to suit several industrial applications by reinforcing with colloidal filler, such as carbon black, which has a large effect on the mechanical properties of rubber. The modified properties of these composites are very complicated depending on a large number of parameters such as size, surface area, structure and dispersion of the carbon particles [1-5].

For a long time simultaneous improvements of seemingly contradictory tire properties, e.g. rolling resistance, wet grip, winter performance and service life have been the major request from automobile manufactures especially for original equipment tires. It was only in the beginning of the nineties that these demands could be met using tread compounds with special polymers and high loadings of silica (together with silanes) instead of carbon black. The properties of these compounds strongly depend on the precipitated silica used.

The stress-strain test is probably still the most widely used test in the rubber industry. Among the purposes for such tests are specification purposes and an over-all quality check on the compound. The mechanical properties of heterogeneous polymeric systems depend on the microstructure of the sample and, for polymer blends, on the size and shape of the domains, and the interactions between the components [6-8].

Bomal et al [9] compared precipitated silicas having different specific surface area and/or dispersibilities. An natural rubber (NR) truck tyre tread with precipitated silica improves rolling resistance, heat generation and high severity wear. High dispersibility precipitated silica is better. Only a partial substitution of carbon black by high specific surface area silica together with adjustment of the formula allows better tread wear performance for all severities together with lower rolling resistance and maintained wet traction.

A variety of solutions to the problem of high temperature stabilization of (NR)/carbon–silica dual phase filler (CSDPF) composites have been compared by Liauw et al [10]. Enhancement in stabilization performance was observed when a small amount of silica was added to a carbon black filled formulation. The stabilization performance was followed via monitoring of loss in tensile strength as a function of ageing time.

In a previous work [11], we have studied effect of the carbon black type, silica content and tensile strain on the positron annihilation lifetime parameters. In this article we investigate the influence of partial replacement of carbon black by precipitated silica, as reinforcing filler for styrene butadiene rubber, on the mechanical properties of these composites. The stress – strain discussion is extended beyond the usual treatment of just uniaxial response to consider the more pragmatic questions of stress softening and hysteresis in rubber composites. The tensile test data for the investigated composites (fresh and pre-extended samples) has been compared with theoretical predictions [12,13].

2. Experimental:

2.1. Materials:

Styrene Butadiene Rubber (SBR) is used as a host material in this study and filled with different ratios of precipitated silica and different types of carbon black. The details of the fillers used and their characteristics are given in Table (1). All samples were prepared according to the recipe presented in table (2). The rubber composites and blends were prepared on a two rolls mill of 300 mm length, 170 mm diameter with speed of slow roll (18 rev. min.) and gear ratio (1.4). After mixing, the rubber compositions were left for about 24 hours

and then molded in an electrically heated hydraulic press at 155 ± 2 ^{o}C under a pressure of 4 MPa and the time of vulcanization was 20 min. The samples were purchased and prepared by using the facilities of The Transport and Engineering (Rubber Manufacturing) Company, Alexandria, Egypt.

Table (1) *Specifications of the filers used for reinforcement.*

Filler	***ASTM designation***	***Average particle size (nm)***	***Surface area (m^2/gm)***	***Structure (cm^3 DBP/100gm)***
ISAF	N220	23	120	115
HAF	N330	29	80	105
FEF	N550	40	42	120
SRF	N770	60	26	70
Precipitated Silica	-	18	170	190

ISAF*: Intermediate super abrasion furnace.* **HAF***: High abrasion furnace.*

FEF*: Fast extrusion furnace.* **SRF***: Semi reinforcing furnace.*

Table (2) *Recipes for SBR composites containing different types of carbon black and different amounts of precipitated silica.*

Ingredients	**Carbon black**				
	Free	N220	N330	N550	N770
SBR (1502)	100	100	100	100	100
Stearic acid	2	2	2	2	2
Zinc oxide	5	5	5	5	5
Sulfur	2.5	2.5	2.5	2.5	2.5
Phenolic aldehyde resin	5	5	5	5	5
MBTS[a]	1.5	1.5	1.5	1.5	1.5
TMTD[b]	0.5	0.5	0.5	0.5	0.5
Titanium dioxide	2	2	2	2	2
Parafinic oil	5	5	5	5	5
Carbon black	0	30	30	30	30
Precipitated silica	varied (0 - 40)	Varied (0 - 40)	varied (0 - 40)	Varied (0 - 40)	varied (0 - 40)

[a] *2-mercapto benzthiozal* [b] *Tetramethylthiuram disulphide*

2.2. Measurements:

Dumbbell shaped samples were cut from the vulcanized sheets by a fine edge steel die of constant width (4 mm). The thickness of the test sample (~1mm) was determined using a dial gauge. The tensile stress-strain properties of rubbers are measured with a home made tensile testing machine. The upper sample grip is attached to a motor which, is used to control the strain rate through a gearbox. The lower sample grip is fixed and connected to a digital force gauge to measure the extension force. The samples were mounted in mechanical clamps 2.5 cm apart, and the crosshead was adjusted to give zero tension. They were stretched at a constant speed (10 mm/min.).

3. Results and Discussions:

3.1. Cyclic Stress – Strain (Hysteresis):

Under cyclic loading, rubber dissipates energy due to hysteresis effects [14], which is caused by a breakdown of crosslinks and a progressive detachment of rubber molecules from the surfaces of reinforcing fillers. Figures (1-3) show the first and second cycles of the viscoelastic cyclic stress-strain of carbon black free samples and samples containing different types of carbon black. As representative example the results of N220- black and N770-black are given.

It is clear that the addition of any type of carbon black with or without silica to (SBR) rubber increases the hysteresis. It is to be noted that, the hysteresis in the (SBR) rubber samples with 30 phr silica is smaller than those with 30 phr carbon black regardless its type. So, one can conclude that the energy required to break the reticulated structure of carbon aggregates and rubber molecules is higher than that needed to overcome the interaction between silica clusters and rubber chain segments.

By comparing the hysteresis in the different samples, one can conclude that: in all (SBR) samples with different types of carbon black as well as those free from carbon black, the hysteresis increases with the content of silica, figures (1-3). At a definite silica concentration, the hysteresis is found to be smaller for the carbon black free (SBR) samples compared to those which are filled with the different types of carbon black. The presence of particulate filler such as carbon black and silica, leads to decreased segmental mobility and hence increased viscosity and internal friction between rubber chains leading to increased hysteresis [15]. This is the result of rearrangement of the molecular structure under applied load and subsequent sliding of chains, past each other. On the other hand, the filler particles tend to form a loose reticulated structure because of their surface activity or mutual interactions. They are also interlaced

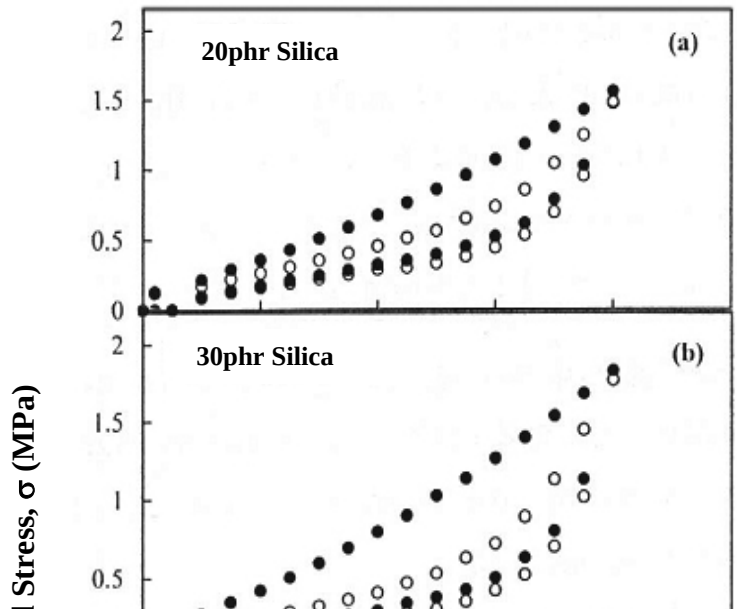

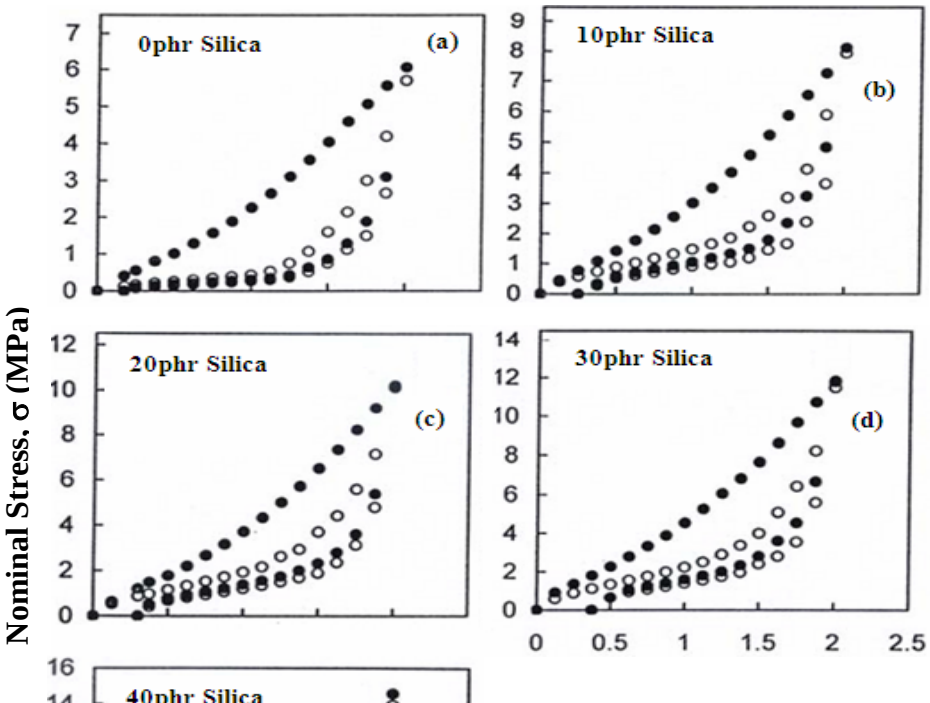
0phr Silica
(a)
10phr Silica
(b)
20phr Silica
(c)
30phr Silica
(d)
40phr Silica
Nominal Stress, σ (MPa)
0
0.5
1
1.5
2
2.5

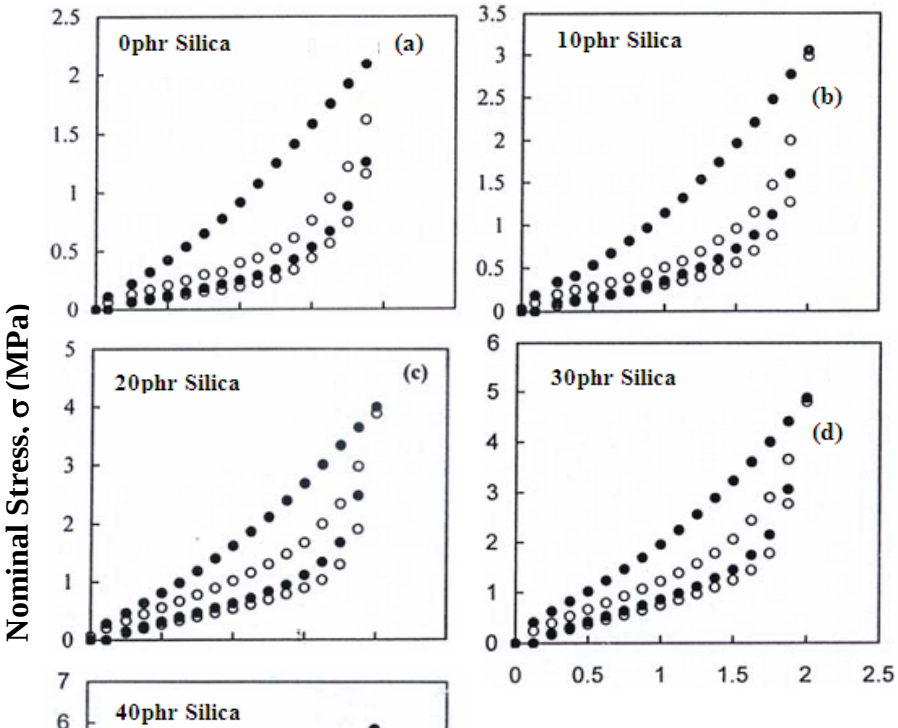
0phr Silica
(a)
10phr Silica
(b)
20phr Silica
(c)
30phr Silica
(d)
40phr Silica
Nominal Stress, σ (MPa)

by the network of rubber chain molecules which are crosslinked during vulcanization. The breakdown of these aggregates, and of the matrix/filler interfacial bonds due to loading, gives rise also to increased hysteresis. In addition, the dispersed hard inelastic filler inclusions or domains in the viscoelastic SBR medium contribute to an increase in the energy loss. Such composites exhibit an inelastic deformation leading to permanent set due to shear yielding and show very high levels of hysteresis [16].

The second cycle hysteresis is smaller than the first cycle one. However, in the third cycle the amount of hysteresis is almost the same as the precedent one. This behaviour is known as stress softening which is due to the modification and reformation of rubber network structures that contribute to weak hysteresis variations. The main features contributing to the stress-softening behaviour involve chemical effects, microstructural damage, multi-chain damage, and micro-void formation [17]. These mechanisms are considerably enhanced by strain amplification caused by rigid particles of carbon black and silica in SBR composites.

The elastic recovery E_R has been calculated for different concentrations of silica in the presence of different types of carbon black. Figure (4a) shows the variations of the elastic recovery E_R with the increase in silica content for carbon free samples and for samples containing different types of carbon black. It is clear that the addition of silica decreases E_R due to permanent yield caused by the redistribution of the broken filler aggregates and the entangling rubber chains. It is also noticed that, the higher the surface area of the carbon black, the smaller is the elastic recovery. This may be attributed to the strong interfacial bonds and the high interaction between carbon blacks of smaller particle size (N220 and N330) and rubber chain segments.

Figures (4b,c) show the variations of the first cycle hysteresis area FA_H and the second cycle hysteresis area SA_H with silica content. Generally, the area of the first hysteresis loop is much larger than that of the second hysteresis loop. This may suggest that the stretching internal friction of the two cycles is quite different and their recovery internal friction is very similar. Both of the FA_H and SA_H increases with the increase in silica concentration due to the decrease in the elasticity of the rubber composites which arises from the physical and chemical crosslinking role of silica in the rubber matrix. The areas of first and second hysteresis loops are also increased with the increase of the carbon black surface area. This may be attributed to the higher internal molecular friction of smaller particle size carbon blacks which retards elastic deformation and increases the energy loss.

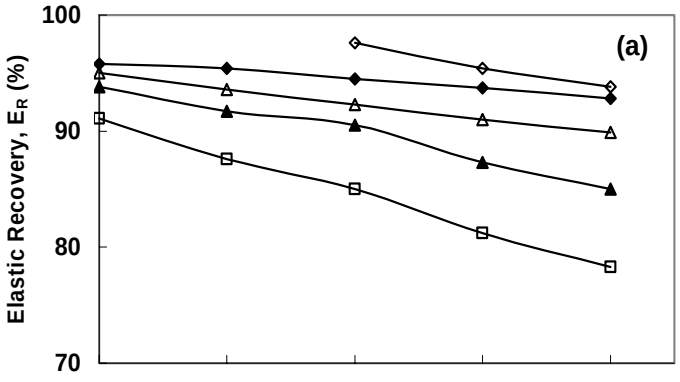

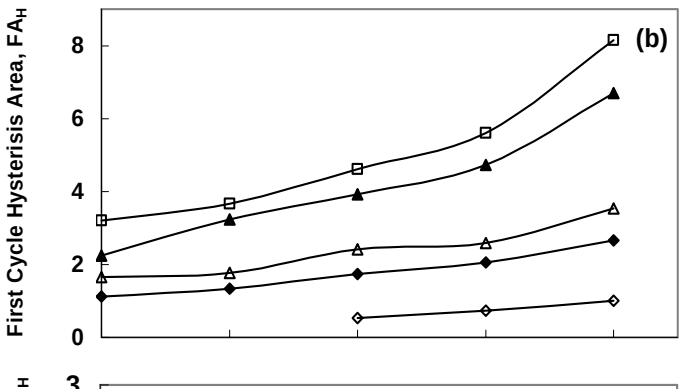

3.3. Application of the Molecular Statistical Model to Virgin and Pre-strained Silica – Carbon Black – SBR Samples

Filler clusters result from an aggregation process in the rubber composite subjected to strong physical bonding between filler particles. With increasing strain of a virgin sample (which received the first extension) a stress-induced successive breakdown of filler clusters takes place, during which the

size of the clusters decreases. This process is almost irreversible, because for cyclic experiments the gaps between broken filler clusters are filled up with rubber that is expected to be strongly bonded to the filler surface and hence, hinders the reaggregation of the clusters when the stress relaxes during the back cycle of straining. It means that the cluster size that is reached at the maximum strain of the first cycle remains fixed for a long period of time and almost no change of the cluster size takes place during the following cycles as long as the maximum pre-strain is not exceeded. If a larger strain is applied in a following cycle, a further breakdown of the clusters appears that is then frozen in the next cycles. This is the basic mechanism of stress softening in filler reinforced rubbers.

The stress-strain curves for simple uniaxial extension can be fitted with the generalized non-Gaussian tube model of finite network extensibility with a topological constraint contribution of the form [18]:

$$\sigma = G_c\left(\lambda-\lambda^{-2}\right)\left\{\frac{1-\frac{T_e}{n_e}}{\left(1-\frac{T_e}{n_e}\left(\frac{\lambda^2+2}{\lambda-3}\right)\right)^2}-\frac{\frac{T_e}{n_e}}{1-\frac{T_e}{n_e}\left(\frac{\lambda^2+2}{\lambda-3}\right)}\right\} + 2G_e\left(\lambda^{-1/2}-\lambda^{-2}\right) \qquad (1)$$

Here λ is the extension ratio, the fitting parameters, $\boldsymbol{G_c}$ is the elastic modulus that corresponds to the crosslink constraints, $\boldsymbol{G_e}$ corresponds to the topological tube constraints, T_e is the Langley trapping factor [19] and n_e is the segment number of chains between successive entanglements.

The stress-strain curves in the second or third cycle can be described by a constant strain amplification factor $X_{max}=X(\varepsilon_{max})$ that depends on the pre-strain ε_{max} as long as the applied external strain ε is smaller than ε_{max}.

$$\lambda = 1+\mathrm{X}_{\max}\varepsilon \qquad for\ \varepsilon \prec \varepsilon_{\max} \qquad (2)$$

The hydrodynamic amplification factor is given by the following scaling law [20]:

$$\mathrm{X} = 1+const.\left(\frac{\xi}{a}\right)^{d_\mathrm{w}-d_f}\varphi^{\frac{2}{d_f-3}} \qquad (3)$$

Here, ξ is the cluster size, a is the particle size, φ is the filler concentration, d_f is the fractal dimension. It is quite remarkable that nearly all carbon blacks and

silicas have a unique surface fractal dimension $d_f \approx 2.6$, in line with the most recent theoretical models for physical concepts of surface growth [21]. The quantity d_w is assumed to be related to the fractal cluster dimension [22] as $d_w = \frac{3}{2} d_f$ .That is the structural parameter d_f characteristic of the volume averaged porosity is linked to the dynamic parameter d_w specifying anomalous diffusion [23]. For common particulate fillers, such as carbon black and silica, the value of the constant in equation (3) ranges from 1.5×10^3 to 1.7×10^3.

The concept of stress induced cluster breakdown leads to an exponential decrease in the cluster size with increasing strain. Then, instead of equation (2) with a constant hydrodynamic amplification factor X_{max}, relevant to pre-strained samples, the equation for the virgin sample has the form:

$$\lambda = 1 + X(\varepsilon)\varepsilon = 1 + X_\infty \varepsilon + (X_o - 1)\exp(-z(1+\varepsilon))\varepsilon \qquad (4)$$

The exponent z is given by $z = \alpha(d_w - d_f)$ and the amplification factors X_o and X_∞ are for the zero and infinite strain limits. The stress-strain behaviour of filler reinforced virgin rubber samples is described by equation (1) together with equation (4), while for pre-strained samples equation (2) has to be applied instead of equation (4).

Figures (5 , 6) show the stress-strain behaviour of carbon black free samples and samples containing different types of carbon black for virgin samples and pre-strained samples. As representative example the results of N220- black are given. Beside, fitted curves are shown as solid lines for the pre-strained samples according to equations (1) and (2). The dependence of the estimated fitting parameters G_c and G_e on the concentration of silica is listed in table (3). The crosslink modulus G_c increases with increasing silica content due to the physical cross-linking introduced by filler particles. While, the topological constraint modulus G_e approaches a constant value that is characteristic for the constant entanglement density of the rubber carbon black matrix. The third parameter (T_e / n_e) is independent of the concentration of silica, but increases with increasing the surface area of carbon black. The increase in (T_e / n_e) can be related to an increase of the trapping factor T_e with

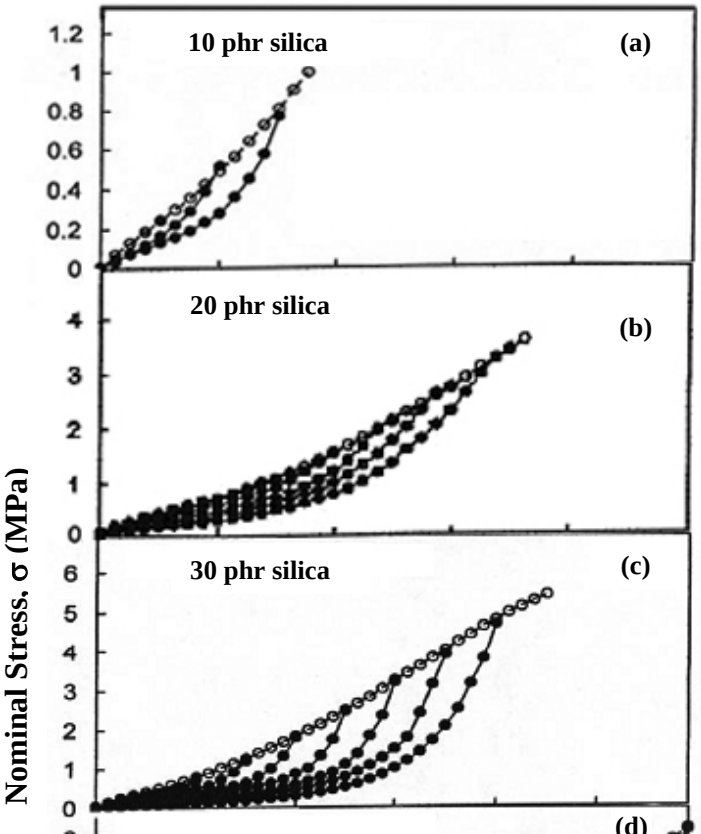

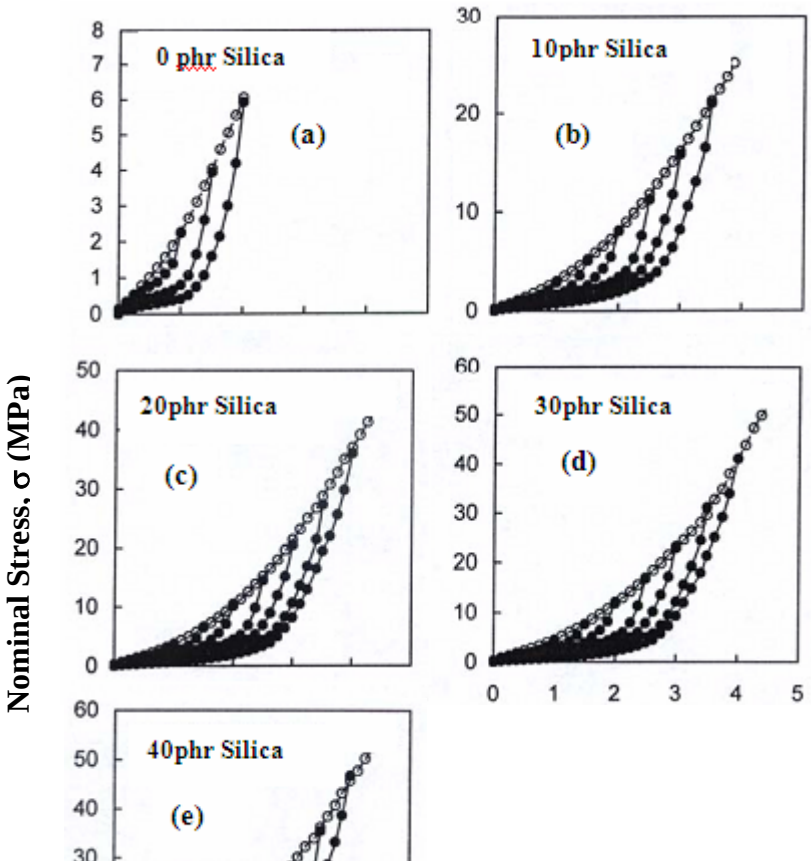
0 phr Silica
(a)
10phr Silica
(b)
20phr Silica
(c)
30phr Silica
(d)
40phr Silica
(e)
Nominal Stress, σ (MPa)

rising crosslink density. The value of (T_e /n_e) varies from 0.006 for N220- black to 0.003 for N770- black. The fitting parameters for the rubber matrix G_c, G_e and (T_e /n_e) are hold constant for the differently pre-strained and virgin samples.

Table(3) *The fitting parameters G_c and G_e Calculated from equation (1).*

	G_c (MPa)

Silica Content (phr)	***C.B- free***	***N770***	***N550***	***N330***	***N220***
0	-	0.39	0.71	1.00	1.33
10	0.13	0.60	0.90	1.32	1.62
20	0.36	0.97	1.33	1.63	1.87
30	0.50	1.11	1.54	1.78	2.09
40	0.67	1.34	1.71	1.96	2.30

	G_e (MPa)				
Silica Content (phr)	***C.B- free***	***N770***	***N550***	***N330***	***N220***
0	-	0.11	0.21	0.35	0.44
10	0.12	0.15	0.26	0.42	0.54
20	0.13	0.16	0.31	0.49	0.61
30	0.14	0.19	0.31	0.50	0.63
40	0.15	0.21	0.34	0.51	0.63

The impact of pre-straining is modellized by the amplification factor X_{max}. Obviously, the fittings for the pre-strained samples with only one variable parameter X_{max} that considers the hydrodynamic reinforcement of differently frozen filler cluster structures are fairly well. A simulation of the first extension of the virgin sample is obtained by the application of equation (1) together with equation (4). This is also shown in figures (5,6) as dashed lines. The fitted values of $X_o, X_\infty and\ z$ are obtained from the linear relations between $\ln(X_{max.} - X_\infty)$ and $(\varepsilon_{max.} + 1)$

Figure (7) depicts the variations of the number of particles per cluster *(ξ/a)*, obtained from equation (3), as a function of the silica content at 100% and 300% strain. The addition of silica increases the number of particles per cluster in the presence of different types of carbon black. The drastic increase in *(ξ/a)* in case of N220 and N330 blacks indicates that there is high interaction between silica and carbon blacks of comparable particle size. This suggests that, the interaction between these two types of carbon black with silica leads to the formation of large clusters containing both fillers. On the other hand, the

relatively small values of *(ξ/a)* in case of N550 and N770 may be due to the coverage of carbon black aggregate with a layer of silica. This also can be observed in the decrease in *(ξ/a)* with strain which is attributed to cluster breakdown, see figure (8).

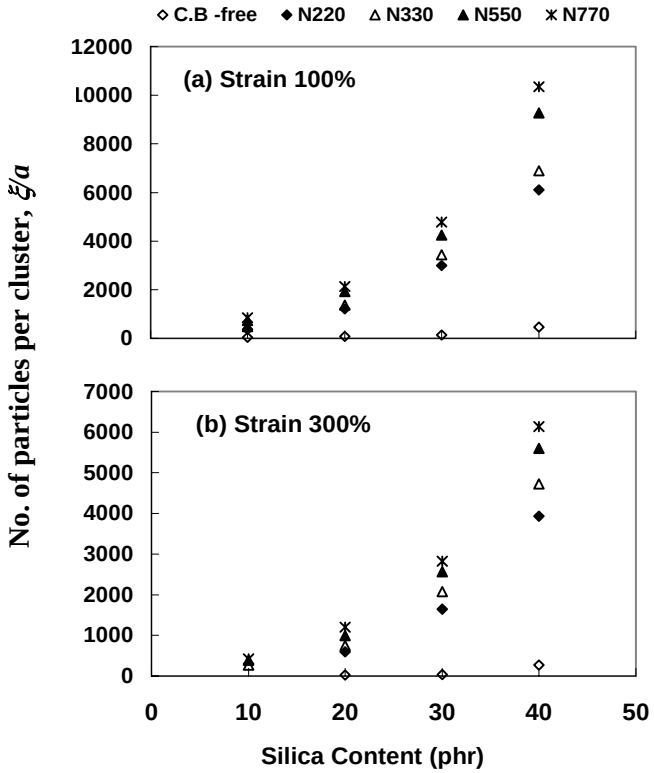

Fig. 7. Variation of the number of particles per cluster in SBR composites with silica content (a) at strain 100% and (b) at strain 300%

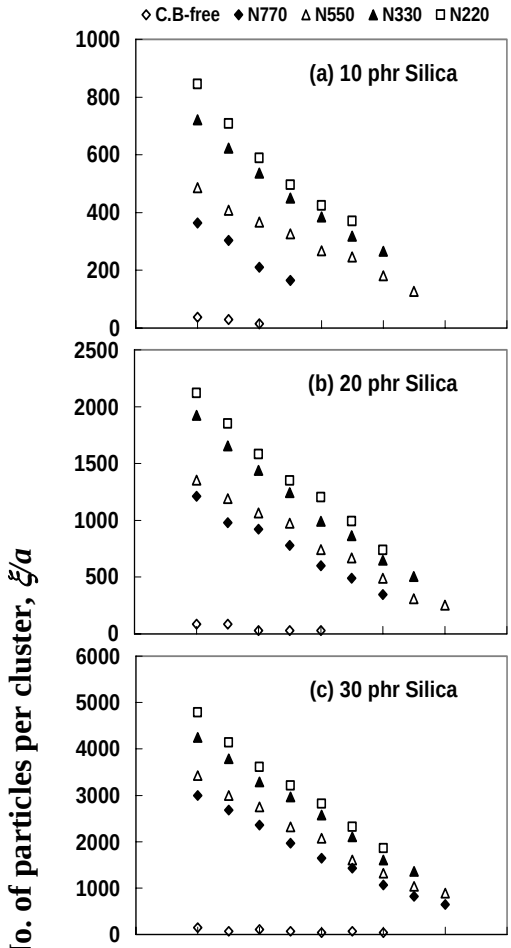

Electron microscopy confirms this idea. Figure (9) shows the SEM photographs for carbon black-silica-SBR composites. It is clear that, a silica layer covers carbon black aggregate only in case of N550 and N770 blacks. While, in the case of N220 and N330 blacks, large clusters of both fillers are observed.

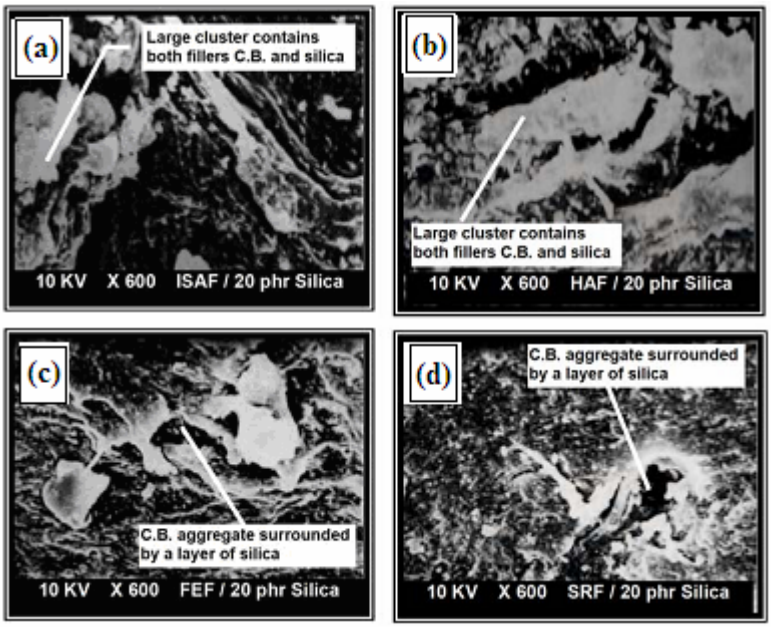

Fig. 9. SEM photographs for composites SBR / 20phr silica loaded with carbon black (a) N220 , (b) N330 , (c) N550 and (d) N770.

4. Conclusion:

The effect of addition of silica on the cyclic stress- strain characteristics of SBR composites loaded with different types of carbon black has been investigated. It was found that, the incorporation of silica increases the hysteresis in the SBR composites. The hysteresis in SBR-carbon black composites was more pronounced than in SBR-silica composites. The elastic recovery (E_R) was found to be dependent on the filler type and content. The stress-strain data for virgin and pre-extended samples has been fitted according to the generalized non-Gaussian tube model of finite network extensibility with a topological constraint contribution taking into account the damage model of stress induced cluster breakdown. New parameters such as the number of particles per cluster have been calculated. A drastic increase in the number of particles per cluster is shown in case of N220 and N330 blacks indicates the high interaction between silica and carbon blacks of comparable particle size which is confirmed with SEM photos.

References:

1. J. P. Donnet and A. Voet, Carbon black physics, chemistry and elastomer reinforcement, New York : Marcel Dekker, (1976).

2. J. P. Donnet and E. Custodero, *Carbon*; **30**, 813 (1992).

3. M. Gerspacher, C.P.Farrell, *Kautsch Gummi Kunstst* **54**, 153 (2001).

4. M. J. Wang, S. Wolff and J.P. Donnet, *Rub.Chem. Tech*.; **64**, 559 (1991).

5. C. M. Blow, Rubber Technology and Manufacture, Institute of Rubber Industry, Butterworthes London, (1971).

6. F. Abd El-Salam, M.H. Abd El-Salam, M.T. Mostafa, M.R. Nagy and M.I. Mohamed, *J. Applied Polymer Science*; **90**, 1539 (2003).

7. A. M. Gessler, *Rub. Chem. Tech*.; **42**, 850 (1969).

8. J. O. Harris and R. W. Wise, Reinforcement of Elastomers. New York: Interscience Publishers, (1965).
9. Y. Bomal, P. Cochet, B. Dejean, I. Gelling and R. Newell, *Kautschuk Gummi Kunststoffe*; **4**: 259 (1998).
10. C. M. Liauw, N.S. Allen, M. Edge, L. Lucchese, *Polym. Deg. Stab*.; **74**, 159 (2001).
11. M. Mohsen, M.H. Abd-El Salam, A. Ashry, A. Ismail and H. Ismail, *Polym. Deg. Stab*.; **87**, 381 (2005).
12. M. Kluppel and J. Schramm, Proceedings: ECCMR; Rotterdam, (1999).
13. S. F. Edwards and T. A. Vilgis, *Polymer*; **27**: 483 (1986).
14. G. Kraus, *Adv. Polym. Sci.;* **8**, 155 (1971).
15. W. Ren, *Colloid Polym. Sci*.; **270**, 990 (1992).
16. J. M. Radok and C. L. Tai, *J. App. Polym. Sci*.; **6**, 518 (1962).
17. J. A. Harwood and A. R. Payne, *J. App. Polym. Sci*.; **10**, 1203 (1966).
18. S. Westermann , M. Kreitschmann, W. Pyckhout-Hintzen, D. Richter, E. Straube, B. Farago, G. Goerigk, *Macromolecules*; **32**, 5793 (1999).
19. N. R. Langley, *Macromolecules*; **1**, 348 (1968).
20. S. Govindjee and J. Simo, *J. Mech. Phys. Sol.;* **39**, 87 (1991).
21. A. L. Barabasi, M. Araujo and H. E. Stanley, *Phys. Rev. Lett*., **68**, 3729 (1992).
22. S. Alexander and R. Orbach, *J. Phys. Lett*., **34**, 625 (1982).
23. A. Klemm, R. Metzler and R. Kimmich, *Phys. Rev*. E **65**, 112 (2002).